Clinical and Experimental Gastroenterology

Dovepress

open access to scientific and medical research

Open Access Full Text Article

ORIGINAL RESEARCH

Gardenia Iridoid Glucosides Protect Against α-Naphthalene Isothiocya-Nate-Induced Cholestatic Rats Through Activation of the FXR-SHP Signaling Pathway

Meng Xu[1,*], Ke Che[1,*], Cong Wang[2,*], Ya-Ru Chen[1], Meng-Yuan Chen[1], Guang-Lei Zhang[1], Hao Yu[3], Hao-Nan Xu[1], Ya-Bao Li[1], Ping Sheng[1], Hao Chen[1]

[1]College of Life and Health Sciences, Anhui Science and Technology University, Fengyang, 233100, People's Republic of China; [2]School of Environmental and Biological Engineering, Nanjing University of Science and Technology, Nanjing, 210094, People's Republic of China; [3]Bozhou University, Bozhou, 236800, People's Republic of China

*These authors contributed equally to this work

Correspondence: Hao Chen; Ping Sheng, Email chenhao@ahstu.edu.cn; astu100@126.com

Introduction: Cholestasis is a common liver disorder that currently has limited treatment options. Gardenia Iridoid Glucosides (GIG) have been found to possess various physiological activities, such as cholagogic, hypoglycemic, antibacterial, and anti-inflammatory effects. The objective of this study was to investigate the effects of GIG on bile acid enterohepatic circulation and explore the underlying mechanism in cholestatic rats.

Methods: In order to identify key pathways associated with cholestasis, we conducted Gene Ontology (GO) Enrichment and Kyoto Encyclopedia of Genes and Genomes (KEGG) analyses. In vivo experiments were then performed on alpha-naphthylisothiocyanate (ANIT)-treated rats to assess the impact of GIG. We measured bile flow and various biomarkers including total bilirubin (TB), total bile acids (TBA), total cholesterol (TC), malondialdehyde (MDA), glutamic-pyruvic transaminase (GPT), glutamic oxaloacetic transaminase (GOT), and total superoxide dismutase (T-SOD) in the serum. We also examined the expression levels of bile salt export pump (BSEP), ATP-binding cassette subfamily B member 4 (ABCB4), far-nesoid X receptor (FXR), small heterodimer partner (SHP), cholesterol 7α-hydroxylase (CYP7A1), and sodium taurocholate cotransporting polypeptide (NTCP) in liver tissue. In vitro experiments were conducted on primary hepatocytes to further investigate the mechanism of action of GIG on the expression of SHP, CYP7A1, NTCP, and FXR.

Results: Our in vivo experiments demonstrated that GIG significantly increased bile flow and reduced the levels of TB, TBA, TC, MDA, GPT, and GOT, while increasing T-SOD levels in ANIT-treated rats. Addi-tionally, GIG ameliorated liver tissue damage induced by ANIT, upregulated the expression of BSEP and ABCB4, and modulated the protein expression of FXR, SHP, CYP7A1, and NTCP in model rats. In vitro experiments further revealed that GIG inhibited the expression of SHP, CYP7A1, and NTCP by suppressing the expression of FXR.

Conclusion: This study provides new insights into the therapeutic potential of GIG for the treatment of cholestasis. GIG demonstrated beneficial effects on bile acid enterohepatic circulation and liver biomarkers in cholestatic rats. The modulation of FXR and its downstream targets may contribute to the mechanism of action of GIG. These findings highlight the potential of GIG as a therapeutic intervention for cholangitis.

Keywords: Gardenia Iridoid Glucosides, FXR, SHP, cholestasis

Introduction

The liver is a vital organ responsible for drug metabolism, detoxification, and synthesis of essential substances, making it a crucial component of the mammalian body's overall function.[1] Cholestasis[2] is a disorder of bile formation that is

Received: 1 September 2023
Accepted: 17 November 2023
Published: 8 December 2023

a leading cause of serious liver disease. Acute hepatitis, viral infection, alcoholic liver disease, and drug-induced liver injury[3] cause it. According to ex-pert consensus, the overall incidence of cholestatic liver disease in patients with chronic liver diseases can be as high as 10.26%.[4] The sustainable development of biliary stasis liver fibrosis[5] can eventually develop into liver fibrosis, liver cirrhosis, or even liver cancer, which can threaten human health. Ursodeox-ycholic acid (UDCA) is the only approved drug for cholestasis treatment, but its overdose can lead to hepatobiliary impairment and cytotoxicity.[6] Therefore, it is imperative to study the pathogenesis and treatment of intrahepatic cholestasis.

Gardenia contains a wide variety of cyclic enol ether compounds, including jinipin glycoside, jinipin acid, gardenia glycoside, and gardenia glycoside. GIG exhibits significant pharmacological activity, including strong laxative and emetic effects.[7] Iridoid Glucosides[8,9] are cyclic enol ether terpene glucosides and serve as the main active ingredient in hepatoprotective and cholagogic agents, which have been shown to upregulate bile transporters and increase bile excretion. Farnesoid X Receptor (FXR) is a member of the orphan nuclear receptor family and nuclear bile acids receptor.[10] It plays a role in bile acid synthesis, regulation within the liver, glucose metabolism, and hepatoprotection. Binding to bile acids, FXR activates the small molecule heterodimer partner (SHP) to form the FXR-SHP functional axis,[11] which significantly regulates bile acid synthesis.

There are many previous researches about cholestasis and Geniposide. Tan et al. Have found that geniposide attenuates alpha-naphthylisothiocyanate-induced intrahepatic cholestasis by downregulating the STAT3 and NF-κB signaling pathways.[12] There is previous research that addressed the effect of geniposide (GE) on ANIT-induced cholestasis and studied the same indications as bile acids biosynthesis was decreased through down-regulation of CYP7A1. It was also found that GE Significantly increased canalicular bile acids secretion via BSEP. Furthermore, the gene and Protein expression analysis demonstrated activation of FXR, and SHP after GE administration.[13] In another research, the mechanisms for BSEP regulation by GE were investigated. GE induced the mRNA levels of BSEP in HepG2 cells and cholestatic mice, and knockdown of FXR and Nrf2 reduced the mRNA expression of BSEP at varying degrees after treatment of GE. FXR acts as the major regulator of BSEP transcription. GE regulated the expression of BSEP through FXR and Nrf2 signaling pathway.[14]

Although there have been numerous studies on cholestasis and Geniposide, research on the Iridoid Glucosides class of compounds remains limited. In this study, we investigated the effects of Iridoid Glucosides from Gardenia on cholestasis, aiming to identify pharmacological components with potentially superior activity and lower costs compared to Geniposide. Additionally, we employed GO enrichment and KEGG network pharmacology analyses to elucidate the key pathways affected by the Iridoid Glucosides mixture in cholestasis. Furthermore, we experimentally validated the accuracy of network pharmacology predictions. Thus, this study, in comparison to prior research, not only expands the repertoire of compounds studied but also integrates the innovative approaches of network pharmacology, aiming to uncover more effective mechanisms and compounds for the treatment of cholestasis in the context of Geniposide.

Materials and Methods

Drugs and Reagents

GIG (No. 200584724M; Geniposide, shanzhiside, Geniposidic acid, Gardenoside content 15.75%, 21.22%, 18.25%, and 10.66%, respectively) was provided by Nanjing Zelang Biological Products Co., Ltd. (Jiangsu, China). Ursodeoxycholic acid (H20210398) was purchased from Losan Pharma GmbH (Germany), α-naphthyl isothiocyanate (ANIT, F1707046) was purchased from Aladdin Reagent (China); glutamic-pyruvic transaminase (GPT, 20210423), glutamic oxaloacetic transaminase (20210424), total superoxide dismutase (20210807) activity and total bilirubin (20210625), total bile acids (20210622), total cholesterol (20211128), malondialdehyde (MDA, 20211127) kits were pur-chased from Nanjing Jiancheng Institute of Biological Engineering (China). Farnesoid X receptor (ab129089), small heterodimer partner (ab300579), cholesterol 7α-hydroxylase (ab65596), sodium taurocholate cotransporting polypeptide (ab131084), ATP-binding cassette subfamily B member 4 (ab272457), bile salt export pump (ab155421) and Glyceraldehyde 3-phosphate dehydrogenase (ab8245) protein antibodies were purchased from Abcam (USA).

Function Enrichment Analysis of Cholestasis

In this study, the gene expression profiles of cholestasis from GEO were selected; and the GSE46960 dataset (Bessho et al, 2014) and GPL6244 platform were downloaded. "Adjusted P<0.05 and Log Fold Change (FC)>1 or Log (FC)<−1" were defined as the threshold for the differentially expressed genes (DEGs), and analysis was performed using the clusterProfiler R package[11] to analyze the GO and KEGG pathways' enrichment.

Animal Experimentation

Male and female Sprague Dawley (SD) rats (240–280 g, 8–10 weeks) were purchased from the Hunan Slaughter Jingda Laboratory Animal Co (Laboratory animal production license No. SCXK (Xiang) 201–0005) and housed in a temperature-controlled room (24 ± 1°C) on a 12 h/12 h light-dark cycle (lights on at 0630) with free access to food and water. Ninety rats were randomly distributed into six groups of 15 rats each: ① normal control group (control); ② ANIT model group (model); ③ GIG low dose group (25 mg/kg/d, GIG-L); ④ GIG medium dose group (50 mg/kg/d, GIG-M); ⑤ GIG high dose group (100 mg/kg/d, GIG-H); ⑥ UDCA group (100 mg/kg/d, UDCA). All the rats received intragastric administration once daily for 14 days, The normal control and ANIT model groups were given 0.5% carboxymethyl cellulose sodium (CMC-Na) by gavage at 10 mL/kg. The cholestasis model was replicated by gavage of ANIT (65 mg/kg) 90 min after the administration on the 12 days, except for the normal control group. All experiments were performed in accordance with the China Public Health Service Guide for the Care and Use of Laboratory Animals. The animal care and experimental procedures were approved by the Animal Ethics Committee of Anhui Science and Technology University (NO.202002). At the end of the experiments, the rats were anesthetized with pentobarbital (80 mg/kg, i.p.), and their necks were dislocated for euthanasia. The doses of GIG were determined from preliminary studies.[9,15,16]

Measurement of Bile Flow

After 1 h of final administration, the rats were anesthetized with an intraperitoneal injection of 20 mg/mL pentobarbital sodium (4 mL/kg), fixed supine on a surgical plate, and the common bile duct was intubated. A PE drainage tube (Smiths Medical Porte Fine Bore LDPE Tubing) was inserted into their common bile duct for approximately 1cm, and bile flow[17] was collected at 1 h, 2 h, 3 h, and 4 h respectively. Bile samples were collected separately during the intervals of 0–1 hour, 1–2 hours, 2–3 hours, and 3–4 hours. Subsequently, a comparison was conducted among the groups for bile flow rates during each specific interval (0–1h, 1–2h, 2–3h, 3–4h) as well as the cumulative flow rate over the entire 4-hour period.

GPT, GOT, T-SOD Activity, TBA, TC, TB, and MDA Contents

Blood was collected from the abdominal aorta, centrifuged at 3500 r/min, and the upper serum was used to determine the GPT, GOT, T-SOD activity and the TBA, TC, TB, and MDA contents using kits according to the manufacturers' instructions.

HE Staining and Immunofluorescence Staining

The animals were euthanized, and livers were collected. The liver samples were embedded in paraffin, coronally sliced at 5-μm, and measured by HE staining and immunofluorescence staining.[18] The primary antibodies were ABCB4 (1:500) and BSEP (1:500). ABCB4 and BSEP, respectively, emit orange red fluo-rescence on the cell membrane using DyLight 594 goat anti rabbit IgG coupled with Alexa fluor, and DyLight 488 goat anti mouse IgG exhibits green fluorescence on the cytoplasm.

Western-Blot

Liver tissues were lysed with RIPA on ice and centrifuged (4°C, 1200 rpm, 15 min), and the supernatant protein concentration was determined by the BCA method. The protein samples were first loaded into 10% sodium dodecyl sulfate-polyacrylamide gel electrophoresis (SDS-PAGE) and transferred to polyvinylidene fluoride (PVDF) membranes.

The membranes were blocked by 5% skimmed milk in TBST for 2 h at room temperature. Subsequently, membranes were probed with primary monoclonal antibodies: FXR (1:1000), SHP (1:1000), CYP7A1 (1:1000), NTCP (1:1000), and GAPDH (1:2000) at 4°C overnight. After washing with TBST, the membranes were incubated with the secondary antibodies at room temperature for 2 h. The protein bands were visualized by enhanced chemiluminescence, with GAPDH as a loading control.

Isolation and Culture of Primary Rat Hepatocytes

Primary hepatocytes were isolated from male adult SD rats (Shanghai SLAC Laboratory Animal Co., Ltd.), maintained in DMEM containing 10% FBS (Gibco). After plating the cells, the medium was replaced 24 h later. The control was the complete medium (Normoxia). Different experimental groups used Dulbecco's modified Eagle's medium supplemented with 0-150 μM (Sigma) or DFO (Sigma). Analysis of cell lysates was done at the indicated times, and cell samples under different treatments were collected and divided into negative control group (NC), Z-GS intervention group (Z-GS), low GIG treatment group (1 mg/L, L-GIG), high GIG treatment group (4 mg/L, H-GIG), H-GIG + Z-GS treatment group (H-GIG+Z-GS), and rat primary hepatocytes were treated with interventions respectively for 3 d according to the grouping requirements except for the NC group. The total proteins were extracted and isolated on the fourth day, and the levels of FXR and SHP proteins in the primary hepatocytes were measured with GAPDH as the reference for gray value analysis.

Statistical Processing

The measurement data were expressed as mean ± SEM. SPSS 25.0 statistical software (IBM SPSS Statistics for Windows, IBM Corp) was adopted for all statistical analyses. We used Student's *t*-test for comparison of two groups and the one-way ANOVA test for comparison of two or more groups.

Results

Function Enrichment Analysis of Cholestasis

In the cholestasis group compared to the normal group, 599 DEGs were found, and 335 upregulated and 264 down-regulated genes were identified (Figure 1A and B). Based on the clusterProfiler R package, a total of 582 GO functions were enriched. DEGs were enriched in a fatty acid metabolic process, and responses to xenobiotic stimulus, nucleotide metabolic process, nucleoside phosphate metabolic process, lipid localization were noted (Figure 1C). In the KEGG pathway enrichment analysis, the 599 DEGs were significantly enriched in 31 signaling pathways (Figure 1D); bile secretion is the key pathway for cholestasis. FXR stimulates bile acids secretion and prevents bile acids reabsorption in the intestine and liver. According to the FXR→SHP→CYP7A1 and NTCP pathway (Figure 1E), bile acids could activate CYP7A1 secretion and inhibit NTCP secretion by binding to FXR. Because geniposidic acid can increase FXR expression, the goal was to find whether geniposidic acid can activate FXR-SHP signaling pathway and anti-cholestasis.

GIG Increases Bile Flow in ANIT-Treated Rats

When compared with the control group, the model group experienced a significant decrease in bile flow (Figure 2, ****$P<0.0001$). Compared with the model group, GIG (25 mg/kg, 50 mg/kg, 100 mg/kg) and UDCA increased the bile flow during the entire time (all but GIG-L in 3~4 h; $P<0.05$ for each comparison).

GIG Affects Serum TBA, TC, TB, MDA, GPT, GOT, and T-SOD in ANIT-Treated Rats

The levels of TBA, TB, TC, MDA, GPT, GOT, and T-SOD in the serum of rats were measured, and the expression of TBA, TB, TC, MDA, GPT, and GOT increased significantly for the model group (Figure 3A–F, $P<0.0001$) compared to the normal control group, except that the level of T-SOD decreased (Figure 3G, $P<0.0001$). The levels of TBA in GIG (25 mg/kg ($P=0.0083$), 50 mg/kg ($P<0.0001$), 100 mg/kg ($P<0.0001$), and UDCA ($P<0.0001$)) were significantly decreased compared to the model group (Figure 3A). The levels of TB in GIG (25 mg/kg ($P<0.0001$), 50 mg/kg ($P<0.0001$), 100 mg/kg ($P<0.0001$)), and UDCA ($P<0.0001$)) were significantly decreased compared to the model group

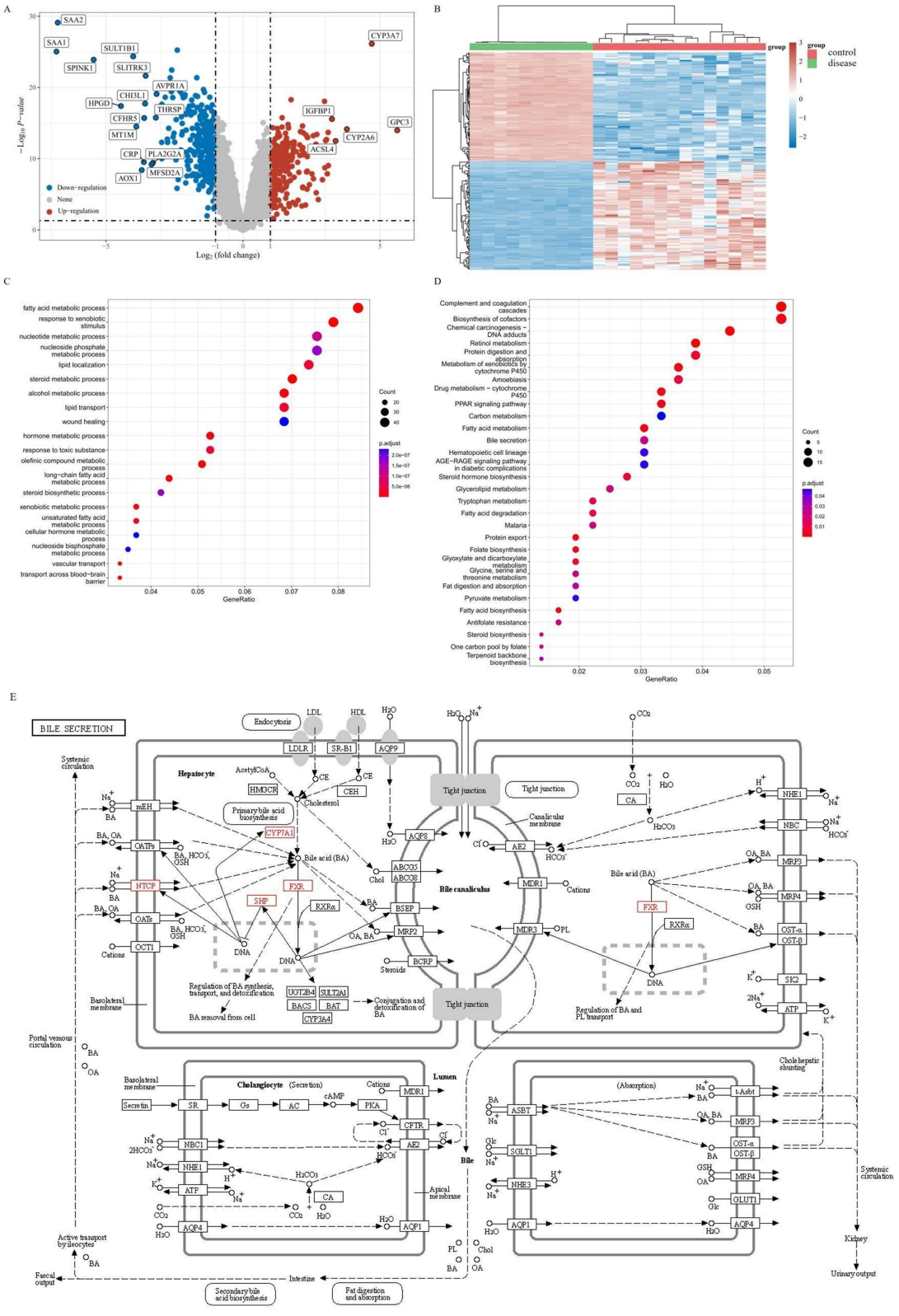

Figure 1 Function enrichment analysis of cholestasis. (**A**) Volcano map of cholestatic DEGs; (**B**) Heat map of cholestatic DEGs; (**C**) GO enrichment of cholestatic DEGs; (**D**) KEGG enrichment of cholestatic DEGs; (**E**) Pathway of bile secretion.

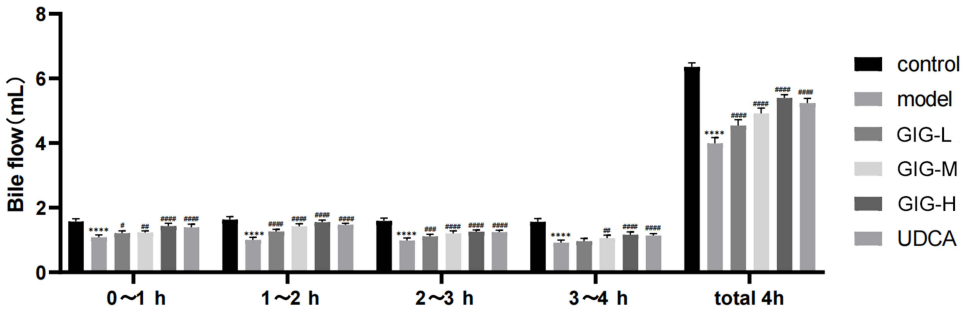

Figure 2 Effect of GIG on bile flow in ANIT-induced rats. Results are shown as mean ± SEM (n=10, n, numbers of rats), compared with the normal control group, ****P<0.0001; compared with the model group, $^{\#}P$<0.05, $^{\#\#}P$<0.01, $^{\#\#\#}P$<0.001, $^{\#\#\#\#}P$<0.0001.

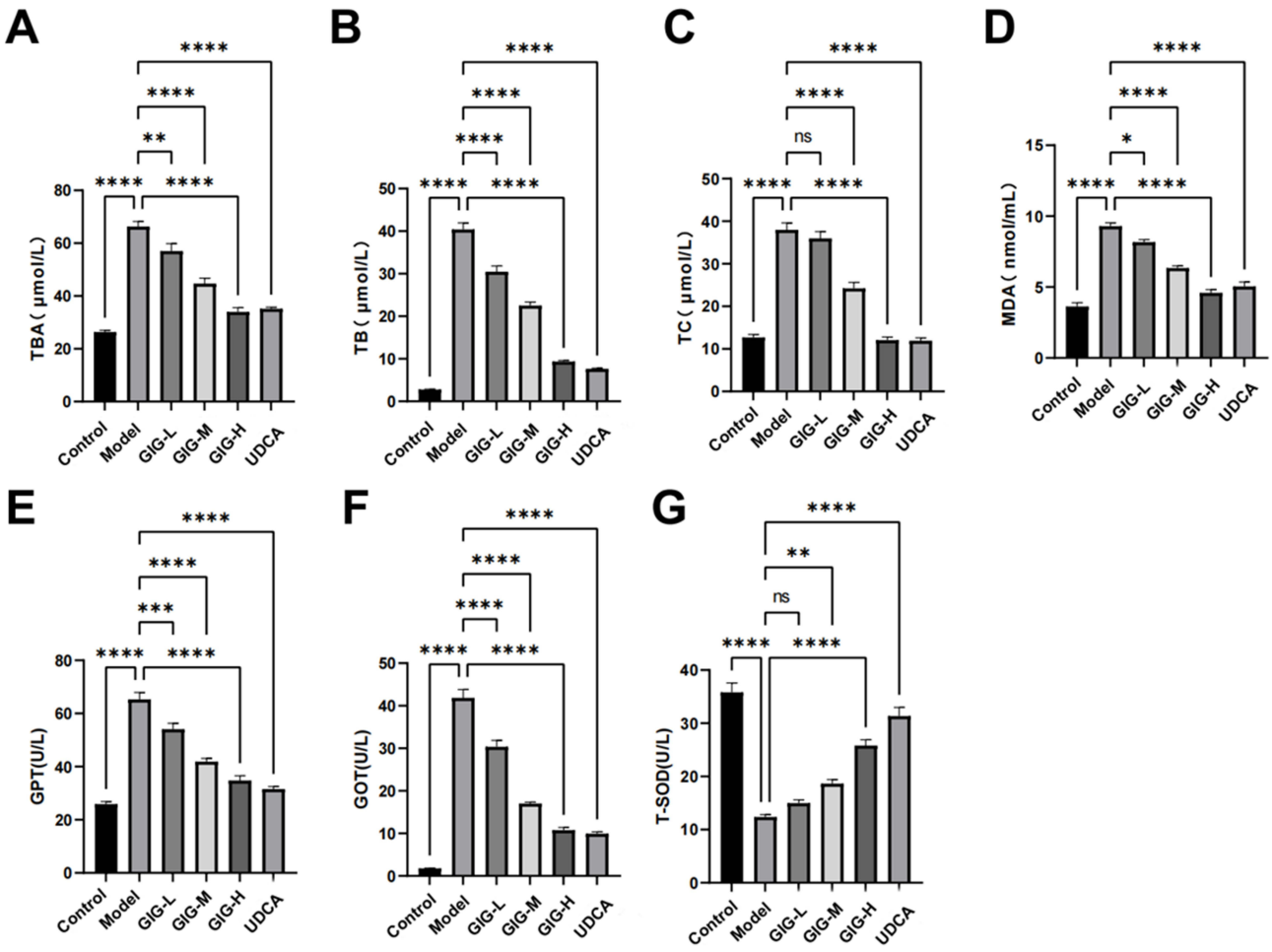

Figure 3 Effects of GIG in ANIT-treated rats inducing TBA, TC, TB, MDA, GPT, GOT, and T-SOD. (**A**) TBA; (**B**) TB; (**C**) TC; (**D**) MDA; (**E**) GPT; (**F**) GOT; (**G**) T-SOD. Results are shown as mean ± SEM (n=10), compared with the other group, *P<0.05, **P<0.01, ***P<0.001, ****P<0.0001.

(Figure 3B). The levels of TC in GIG (50 mg/kg (P<0.0001), 100 mg/kg (P<0.0001)), and UDCA (P<0.0001)) were significantly decreased compared to the model group (Figure 3C). The levels of MDA in GIG (25 mg/kg (P=0.0185), 50 mg/kg (P<0.0001), 100 mg/kg (P<0.0001), and UDCA (P<0.0001)) were significantly decreased compared to the model group (Figure 3D). The levels of GPT in GIG (25 mg/kg (P=0.0004), 50 mg/kg (P<0.0001), 100 mg/kg (P<0.0001)), and UDCA (P<0.0001)) were significantly decreased compared to the model group (Figure 3E). The levels of GOT in GIG (25 mg/kg (P<0.0001), 50 mg/kg (P<0.0001), 100 mg/kg (P<0.0001)), and UDCA (P<0.0001)) were

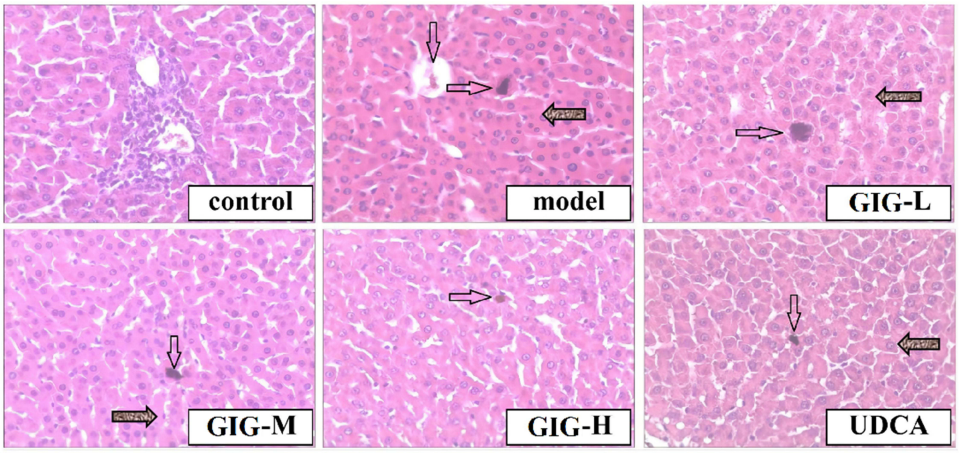

Figure 4 The protective effects of GIG in ANIT-treated rats inducing histopathological observation. The black dot indicated by the arrow represents bile spillover (HE×100). The blank arrow indicates Bile spillover, while the shaded arrow points to cellular swelling.

significantly decreased compared to the model group (Figure 3F). The levels of T-SOD in GIG (50 mg/kg (P=0.0054), 100 mg/kg (P<0.0001)), and UDCA (P<0.0001)) were significantly increased compared to the model group (Figure 3G).

GIG Alleviates Pathomorphological Changes in ANIT-Treated Rats

In the normal control group, the rat liver tissue had a regular cell arrangement, no cell vacuoles or in-flammatory cells in the confluent area, and no abnormalities such as bile overflow (Figure 4). In the model group, the rat liver tissue was swollen and yellowish, with rounded edges, cell vacuoles of different sizes, and a large amount of bile overflow in the confluent area (Figure 4). GIG intervention significantly improved the liver cell's swelling and yellowing, during which the cell vacuoles were relatively reduced in the GIG low and medium dose groups. Only some bile overflowed in the confluent area. In the GIG low and medium dose groups, there were relatively fewer vacuoles, but still, some bile overflowed from the confluent area. The comparison of scores for each group is visible in Table 1. In contrast, in the GIG high dose group, the vacuoles were significantly reduced, the cells were arranged regularly, and basically, no bile overflowed, and marked improvement in cellular swelling.

Effect of GIG on ABCB4 and BSEP Protein Expression in ANIT-Treated Rats

Compared with the normal control group, there was almost the low expression of ABCB4 and BSEP in the model group's liver tissues (Figure 5). Compared with the model group, the expression of BSEP and ABCB4 increased significantly in the GIG middle and high dose groups, and the changes of BSEP and ABCB4 expression showed a positive correlation with the dose of GIG (Figure 5). The expression trends of ABCB4 and BSEP in each group can be seen in Figures 5B and C.

Table 1 The Results of Liver Histopathological Examination Grade. (n=15)

Group	Cellular Swelling	Bile Spillover
Control	–	–
Model	+++	+++
GIG-L	++	++
GIG-M	+	++
GIG-H	–	+
UDCA	–	–

Notes: –, negative; +, slight; ++, moderate; +++, severe.

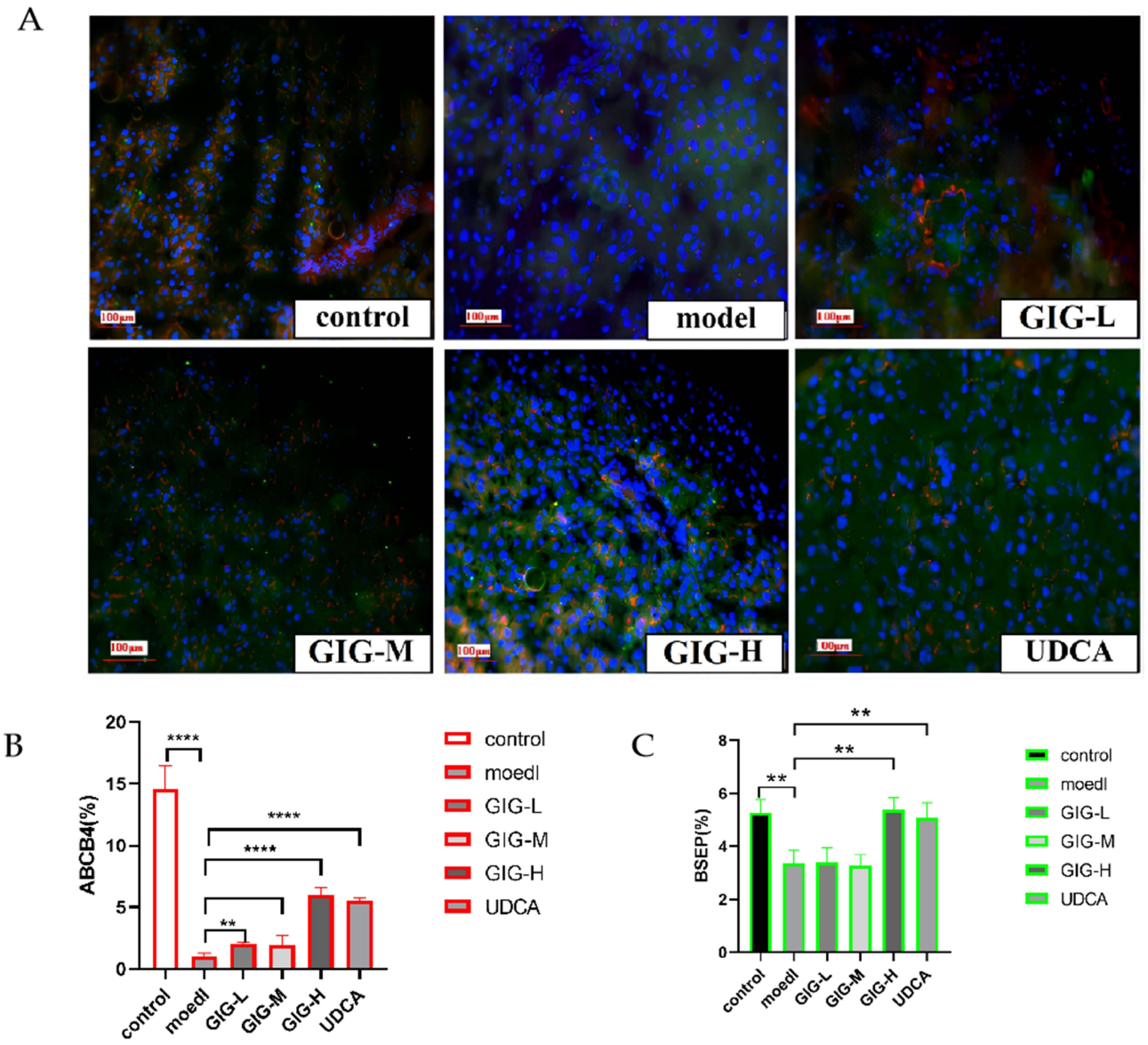

Figure 5 (**A**) Immunofluorescence staining of GIG on expression of ABCB4 and BSEP in ANIT-treated rats' liver tissues. (**B**) The relative percentage of ABCB4 expression. (**C**) The relative percentage of BSEP expression. Red represents ABCB4, and green represents BSEP. ***P*<0.01, *****P*<0.0001.

GIG Affects the Expression of FXR, SHP, CYP7A1, and NTCP in ANIT-Treated Rat Liver Tissue

The protein expressions of NTCP in GIG (25 mg/kg (*P*<0.0001), 50 mg/kg (*P*<0.0001), 100 mg/kg (*P*<0.0001)) and UDCA (*P*<0.0001) were significantly increased compared to the model group (Figure 6). The protein expressions of CYP7A1 in GIG (25 mg/kg (*P*=0.0009), 50 mg/kg (*P*<0.0001), 100 mg/kg (*P*<0.0001)) and UDCA (*P*<0.0001) were significantly decreased compared to the model group (Figure 6).

GIG Affects the Protein Expression of SHP and CYP7A1 in Primary Hepatocytes After FXR Inhibition

SHP expression was significantly suppressed (Figure 7, *P*<0.0001), and CYP7A1 expression was significantly increased (Figure 7, *P*<0.0001) in the Z-GS-treated group compared to the NC group. The pro-tein expressions of SHP in GIG (1 mg/L (*P*<0.0001), 4 mg/L (*P*<0.0001)) were significantly increased compared to the Z-GS group (Figure 7). The protein expressions of CYP7A1 in GIG (1 mg/L (*P*=0.0002), 4 mg/L (*P*<0.0001)) were significantly decreased compared

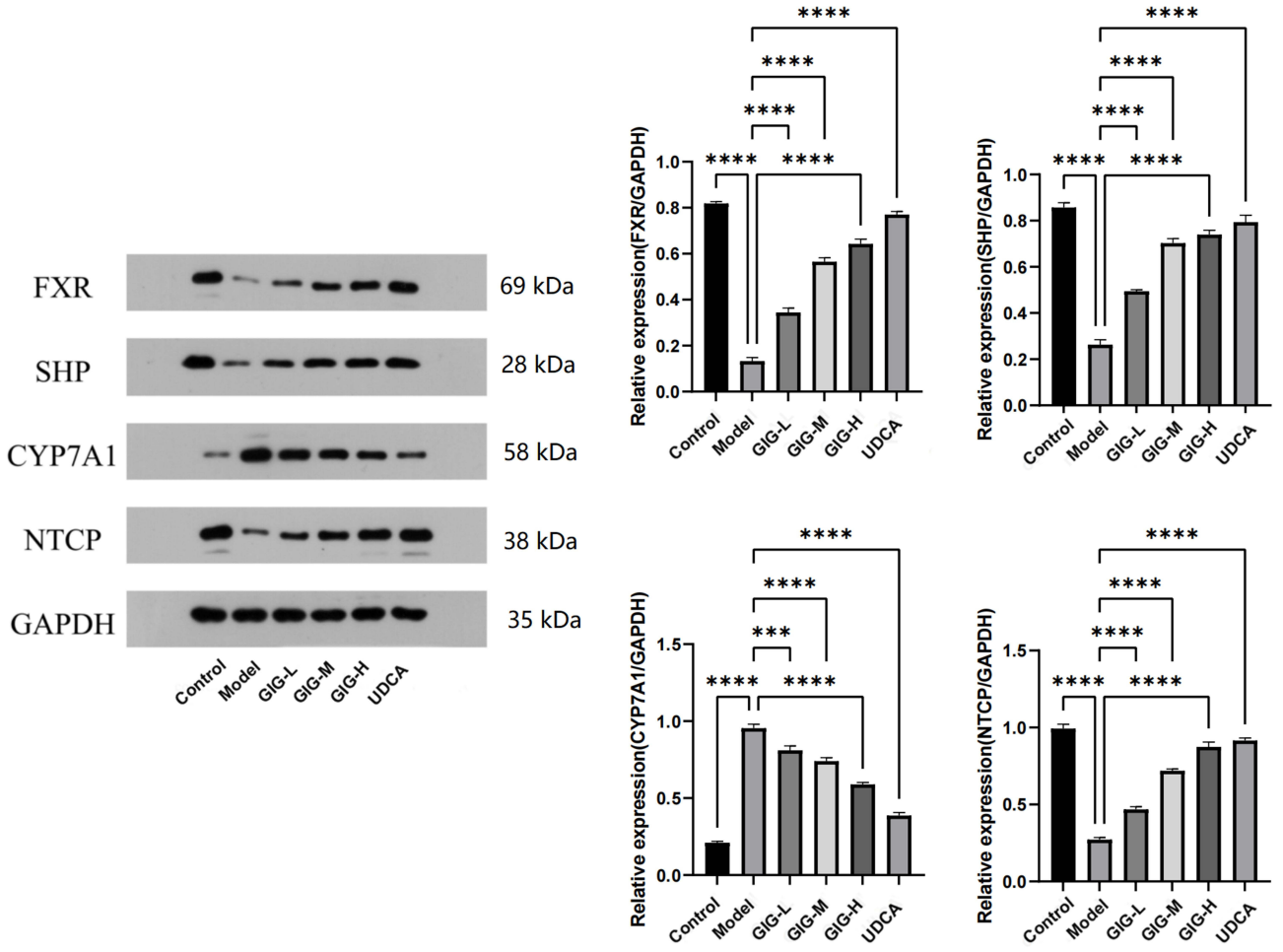

Figure 6 Effect of GIG on the ANIT-treated rat liver tissue inducing the protein expression of FXR, SHP, CYP7A1, and NTCP. Results are shown as mean ± SEM (n=5), compared with the other group, ***P<0.001, ****P<0.0001.

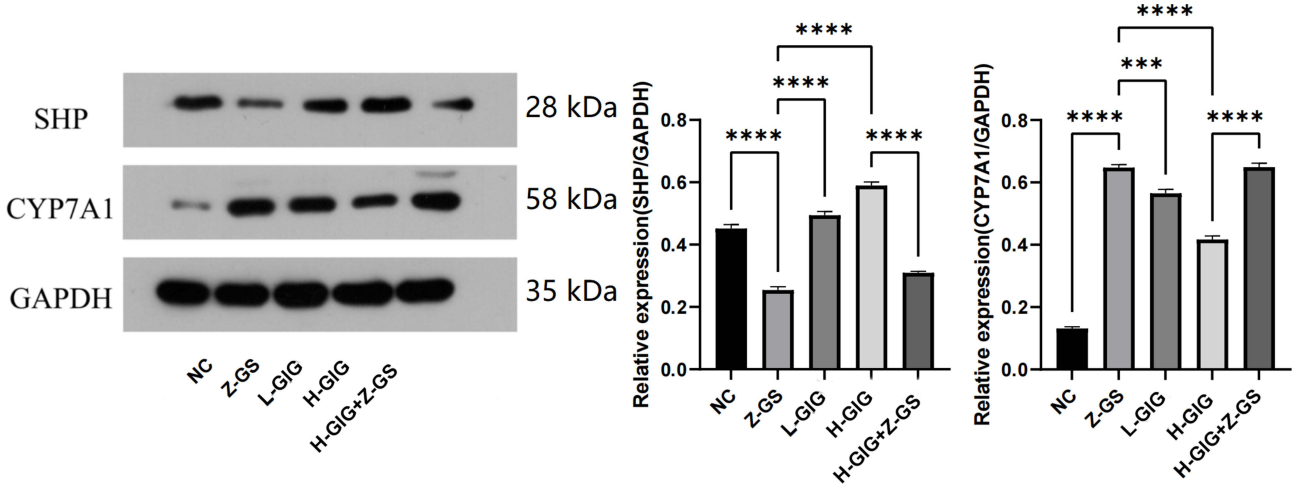

Figure 7 Protein expression of SHP and CYP7A1 in primary hepatocytes. Results are shown as mean ± SEM (n=5), compared with the other group, ***P<0.001, ****P<0.0001.

to the Z-GS group (Figure 7). After using Z-GS, the GIG (4 mg/L) effects on the protein expression of SHP (Figure 7, $P<0.0001$) and CYP7A1 (Figure 7, $P<0.0001$) were reversed.

Discussion

This research investigated the protective effects of GIG on ANIT-induced cholestasis in rats, and ex-plored the potential mechanisms involving the FXR-SHP signaling pathway. Our study provides valuable insights into potential therapeutic strategies for cholangitis. Due to the high incidence of cholestasis and the limited treatment options currently available, the development of effective treatment methods for cholestasis is crucial. This study focused on the use of GIG, a compound known to have various physiological activities such as bile excretion, hypoglycemic, antibacterial, and anti-inflammatory effects. Our study demonstrated that GIG has a protective effect against ANIT-induced liver injury and cholestasis, and may provide a new strategy for the treatment of cholestasis-related liver diseases.

In mammals, oxidation and antioxidant activities are balanced. Oxidative stress mainly occurs due to excessive production of reactive oxygen species or insufficient elimination, and MDA is an important in-dicator of oxidative damage.[19] The end product of lipid peroxidation, MDA, is highly mutagenic.[20] This includes the production of T-SOD,[21] which is the first line of defense against oxidative stress. It is an enzyme-catalyzed antioxidant defense mechanism that can degrade O_2, decompose H_2O_2, and effectively protect cells from damage. This study found that MDA levels in the serum of ANIT-treated rats significantly decreased and T-SOD levels increased with GIG treatment.

In addition, GOT and GPT are important enzyme markers.[22] Increased concentrations of GOT and GPT are associated with liver injury. Liver cells convert cholesterol into bile acids, which are secreted into the intestinal tract through the bile duct system. Furthermore, lipoprotein metabolism requires normal bile acid function and bile production. Elevated total bile acid levels are associated with impaired enterohepatic circulation. The level of total bilirubin reflects the liver's ability to transfer bilirubin from plasma to bile, and increased total bilirubin levels may indicate hemolysis or liver dysfunction. The method of removing cholesterol from the body is through the conversion of cholesterol into bile acids in the liver and excretion of cholesterol into the bile duct through bile acids.[23] In this study, the levels of serum TBA, TB, TC, GPT, and GOT initially increased and bile flow decreased in ANIT-treated rats. Treatment with GIG significantly increased bile flow and decreased serum TBA, TB, TC, GPT, and GOT levels in ANIT-treated rats. HE staining results showed that GIG significantly reduced hepatocyte swelling and inflammatory cell infiltration. These results suggest that potentially, GIG has a protective effect against cholestatic liver in-jury.

To further explore the potential therapeutic significance of GIG in cholangitis, we performed functional enrichment analysis on the gene expression profiles related to cholestasis. The analysis revealed enriched GO terms and KEGG pathways associated with cholestasis. These findings contribute to a better understanding of the molecular pathways involved in cholestasis and provide a basis for future therapeutic interventions. Among the molecular pathway results, we found that bile secretion is the key pathway for cholestasis. Through further analysis of bile secretion, we selected the FXR→SHP→CYP7A1 and NTCP pathways as the main mechanisms for our study.

GIG treatment improved ANIT-induced pathological liver tissue damage and increased the expression of BSEP and ABCB4 in the rat liver model. BSEP and ABCB4 are important bile transport proteins in-volved in bile excretion. The upregulation of these transport proteins by GIG indicates its potential in enhancing bile flow and reducing cholestasis. Furthermore, we investigated the molecular mechanisms un-derlying the protective effect of GIG on cholestasis. In in vitro experiments conducted on primary liver cells, the GIG component Z-GS inhibited the expression of FXR, SHP, CYP7A1, NTCP in hepatocytes. FXR is a nuclear bile acid receptor that plays a critical role in bile acid synthesis and regulation in the liver. Our study demonstrates that GIG activates the FXR-SHP signaling pathway, inhibits bile acid synthesis, and upregulates the expression of bile transport proteins, thereby promoting bile flow and reducing cholestasis. This is consistent with previous research findings that Geniposide acted as an FXR activator to regulate the expression of BSEP. Meanwhile, another study found that bile acid-activated FXR induced BSEP and organic solute transporter beta (OSTβ), and through inducing SHP, it inhibited CYP7A1. Geniposide can regulate transporters and enzymes involved in bile acid homeostasis to reduce the uptake and synthesis of basolateral bile acids while increasing bile acid excretion to counteract the accumulation of bile acids in hepatocytes, thereby exerting a protective effect against ANIT-induced liver injury. Overall, our experiments are consistent with previous research results, demonstrating that GIG-like compounds

have a significant ameliorative effect on cholestasis. Further research is needed to investigate the effects of compounds other than Geniposide.

Through the previous analysis, we found that the pathways selected by GO enrichment and KEGG analysis are consistent with the pathways and targets of cholestasis. This further demonstrates the effectiveness of GO enrichment and KEGG analysis in identifying disease pathways and targets, and suggest that the cycloartane glycoside structures in GIG-like compounds may have therapeutic effects on cholestasis. However, further experimental verification is needed through molecular docking simulations and isolation of monomers.

Conclusion

Our study demonstrates that GIG exhibit significant protective effects against ANIT-induced cholestasis in rats. GIG treatment effectively improves bile flow, reduces liver injury, and promotes the expression of important bile transporters, BSEP and ABCB4, in the liver. These effects are mediated through the activation of the FXR-SHP signaling pathway. Overall, our findings suggest that GIG has potential therapeutic implications for the treatment of cholangitis and cholestasis-related liver diseases. The reliability of the network pharmacology approach is also illustrated.

However, it is important to acknowledge the limitations of our study. Firstly, our research focused on animal models, and further studies are needed to investigate the effects of GIG in human subjects. Addi-tionally, in the mechanism study, we only investigated the impact of GIG on the FXR-SHP axis after the addition of Z-GS in cellular research. The evidence from this exploration is not yet sufficient. In future studies, we plan to knock down key genes to further verify the mechanism of GIG on the FXR-SHP axis. Moreover, as GIG is a mixture, we can separate this mixture into monomers for further research to identify the pharmacologically active components with lower toxicity.

In conclusion, while our study demonstrates the therapeutic potential of GIG in cholestasis, further research is necessary to fully elucidate its mechanisms of action and evaluate its clinical applicability. Addressing these limitations will contribute to a better understanding of GIG's therapeutic value and facilitate its development as a promising treatment option for cholangitis and cholestasis-related liver diseases.

Author Contributions

All authors made a significant contribution to the work reported, whether that is in the conception, study design, execution, acquisition of data, analysis and interpretation, or in all these areas; took part in drafting, revising or critically reviewing the article; gave final approval of the version to be published; have agreed on the journal to which the article has been submitted; and agree to be accountable for all aspects of the work.

Funding

This study was supported by the Project of Natural Science Foundation of Anhui Province (2008085QH395), the major natural science research projects in Anhui Universities (KJ2020ZD011), the Anhui province university outstanding young talent support project (Gxyq2021198), research and development of a feed additive for respiratory diseases and immune enhancement in broilers (horizontal cooperation project: 881383),research on the development of antioxidant functional tea and B2C operation mode technology (horizontal cooperation project: 881384).

Disclosure

Meng Xu, Ke Che, and Cong Wang are co-first authors for this study. The authors report no conflicts of interest in this work.

References

1. Reinke H, Asher G. Circadian clock control of liver metabolic functions. *Gastroenterology*. 2016;150(3):574–580. doi:10.1053/j.gastro.2015.11.043
2. Jenniskens M, Langouche L, Vanwijngaerden YM, Mesotten D, Van den Berghe G. Cholestatic liver (dys)function during sepsis and other critical illnesses. *Intensive Care Med*. 2016;42(1):16–27. doi:10.1007/s00134-015-4054-0
3. Bresnahan E, Ramadori P, Heikenwalder M, Zender L, Lujambio A. Novel patient-derived preclinical models of liver cancer. *J Hepatol*. 2020;72(2):239–249. doi:10.1016/j.jhep.2019.09.028

4. Lu L; Chinese Society of Hepatology and Chinese Medical Association. Guidelines for the management of cholestatic liver diseases (2021). *J Clin Transl Hepatol*. 2022;10(4):757–769. doi:10.14218/JCTH.2022.00147
5. Yi YX, Ding Y, Zhang Y, Ma NH, Shi F, Kang P. Yinchenhao decoction ameliorates alpha-naphthylisothiocyanate induced intrahepatic cholestasis in rats by regulating Phase II metabolic enzymes and transporters. *Front Pharmacol*. 2018;9:510. doi:10.3389/fphar.2018.00510
6. Harada M, Tenmyo N, Aburada M, Endo T. Phagmacological studies of gardeniae fructus. I. Effect of geniposide and genipin on the biliary excretion, the gastric juice secretion, and the gastric contraction, and other pharmacological actions (author's transl). *Yakugaku Zasshi*. 1974;94 (2):157–162. doi:10.1248/yakushi1947.94.2_157
7. Shan M, Yu S, Yan H, Guo S, Xiao W, Wang Z. A review on the phytochemistry, pharmacology, pharmacokinetics and toxicology of geniposide, a natural product. *Molecules*. 2017;22(10):1689. doi:10.3390/molecules22101689
8. Chen H, Huang X, Min J, Li W, Zhang R, Zhao W. Geniposidic acid protected against ANIT-induced hepatotoxity and acute intrahepatic cholestasis, due to Fxr-mediated regulation of Bsep and Mrp2. *J Ethnopharmacol*. 2016;179:197–207. doi:10.1016/j.jep.2015.12.033
9. Pu J, Yuan A, Shan P, Gao E, Wang X, Wang Y. Cardiomyocyte-expressed farnesoid-X-receptor is a novel apoptosis mediator and contributes to myocardial ischaemia/reperfusion injury. *Eur Heart J*. 2013;34(24):1834–1845. doi:10.1093/eurheartj/ehs011
10. Huang X, Wang B, Chen R, Zhong S, Gao F, Zhang Y. The nuclear farnesoid X receptor reduces p53 ubiquitination and inhibits cervical cancer cell proliferation. *Front Cell Dev Biol*. 2021;9:583146. doi:10.3389/fcell.2021.583146
11. Yu G, Wang LG, Han Y, He QY. clusterProfiler: an R package for comparing biological themes among gene. *OMICS: A Journal of Integrative Biology*. 2012;16(5):284–287. doi:10.1089/omi.2011.0118
12. Tan Z, Liu A, Luo M. Geniposide inhibits alpha-naphthylisothiocyanate-induced intrahepatic cholestasis: the down-regulation of STAT3 and NFκB signaling plays an important role. *Am J Chin Med*. 2016;44(4):721–736. doi:10.1142/S0192415X16500397
13. Wang L, Wu G, Wu F, Jiang N, Lin Y. Geniposide attenuates ANIT-induced cholestasis through regulation of transporters and enzymes involved in bile acids homeostasis in rats. *J Ethnopharmacol*. 2017;196:178–185. doi:10.1016/j.jep.2016.12.022
14. Wu G, Wen M, Sun L. Mechanistic insights into geniposide regulation of bile salt export pump (BSEP) expression. *RSC Advances*. 2018;8 (65):37117–37128. doi:10.1039/c8ra06345a
15. Chen H, Li J, Hu L, et al. Effect of geniposidic acid on hepato-enteric circulation in cholestasis rats through Sirt1-FXR signaling pathway. *Zhongguo Zhong Yao Za Zhi*. 2019. 44(4):787–795. Chinese. PMID: 30989893. doi:10.19540/j.cnki.cjcmm.20181204.013
16. Chen H, Gao X, Zhao W, Yu H, Wang N, Mi S. Effect of geniposidic acid on SHP-LRH-1 signaling pathway in cholestasis rats. *Zhong Nan Da Xue Xue Bao Yi Xue Ban*. 2019;44(6):605–613. doi:10.11817/j.issn.1672-7347.2019.06.001
17. Zou Z, Hu X, Luo T, Ming Z, Chen X, Xia L. Naturally-occurring spinosyn A and its derivatives function as argininosuccinate synthase activator and tumor inhibitor. *Nat Commun*. 2021;12(1):2263. doi:10.1038/s41467-021-22235-8
18. Ward LD, Tu HC, Quenneville CB, Tsour S, Flynn-Carroll AO, Parker MM. GWAS of serum ALT and AST reveals an association of SLC30A10 Thr95Ile with hypermanganesemia symptoms. *Nat Commun*. 2021;12(1):4571. doi:10.1038/s41467-021-24563-1
19. Fujita N, Nishie A, Asayama Y, Ishigami K, Ushijima Y, Takayama Y. Fibrosis in nonalcoholic fatty liver disease: noninvasive assessment using computed tomography volumetry. *World J Gastroenterol*. 2016;22(40):8949–8955. doi:10.3748/wjg.v22.i40.8949
20. Blesl A, Jüngst C, Lammert F, Fauler G, Rainer F, Leber B. Secondary sclerosing cholangitis in critically ill patients alters the gut-liver axis: a case control study. *Nutrients*. 2020;12(9):2728. doi:10.3390/nu12092728
21. Liu Y, Li A, Feng X, Sun X, Zhu X, Zhao Z. Pharmacological investigation of the anti-inflammation and anti-oxidation activities of diallyl disulfide in a rat emphysema model induced by cigarette smoke extract. *Nutrients*. 2018;10(1):79. doi:10.3390/nu10010079
22. Chong CLG, Hussan F, Othman F. Hepatoprotective effects of morinda citrifolia leaf extract on ovariectomized rats fed with thermoxidized palm oil diet: evidence at histological and ultrastructural level. *Oxid Med Cell Longev*. 2019;2019:9714302. doi:10.1155/2019/9714302
23. Shi Z, Li T, Liu Y, Cai T, Yao W, Jiang J. Hepatoprotective and anti-oxidative effects of total flavonoids from Qu Zhi Qiao (Fruit of Citrus Paradisi cv. Changshanhuyou) on nonalcoholic steatohepatitis in vivo and in vitro through Nrf2-ARE signaling pathway. *Front Pharmacol*. 2020;11:483. doi:10.3389/fphar.2020.00483